Blend electrospinning of dye-functionalized chitosan and poly(ε-caprolactone): towards biocompatible pH-sensors†

Ella Schoolaert,[a] Iline Steyaert,[a] Gertjan Vancoillie,[b] Jozefien Geltmeyer,[a] Kathleen Lava,[b] Richard Hoogenboom*[b] and Karen De Clerck*[a]

Fast-response and easy-to-visualize colorimetric nanofibrous sensors show great potential for visual and continuous control of external stimuli. This makes them applicable in many fields, including wound management, where nanofibers serve as an optimal support material. In this paper, fast responding and user-friendly biocompatible, halochromic nanofibrous sensors are successfully fabricated by incorporating the halochromic dyes Methyl Red and Rose Bengal inside a chitosan/poly(ε-caprolactone) nanofibrous matrix. The commonly applied dye-doping technique frequently suffers from dye-leaching, which not only reduces the sensor's sensitivity over time but can also induce adverse effects. Therefore, in this work, dye-immobilization is accomplished by covalent dye-modification of chitosan before blend electrospinning. It is shown that efficient dye-immobilization with minimal dye-leaching is achieved within the biomedical relevant pH-region, without significantly affecting the halochromic behavior of the dyes. This is in contrast to the commonly applied dye-doping technique and other dye-immobilization strategies stated in literature. Moreover, the nanofibers show high and reproducible pH-sensitivity by providing an instantaneous color change in response to change in pH in aqueous medium and when exposed to acidic or basic gases. The results stated within this work are of particular interest for natural (bio)polymers for which covalent modification combined with electrospinning provides a universal method for versatile dye-functionalization of large area nanofibrous membranes with proper dye-immobilization.

Introduction

Halochromic dyes possess a pH-sensitive chromophore, which makes them respond to pH-changes in the environment by a color change visible to the naked eye. Thanks to this fast, simple and easy read out signaling function, such pH-indicators are frequently applied in many fields, including analytical chemistry, biology, food chemistry, water treatment, cosmetics and biomedical applications.[1–3] Halochromic dyes also show high potential for the development of so-called smart materials, *i.e.* materials that are able to sense and respond to changes in their environment. A smart halochromic sensor can be designed by incorporating the halochromic dye into a specific matrix with a desired structure, resulting in a custom material that signals pH-changes through a fast and simple change of color.[4,5]

Such chromic materials play an important role in user-friendly products, providing clear information in a non-destructive way. One of the areas where halochromic sensors could be of great use, is the biomedical field. For wound management, in particular, pH is a major parameter being researched, since it is a biological marker for both healing and infection.[6–10] A halochromic wound dressing would, therefore, be able to assess the condition of the wound and indicate whether the wound dressing has to be replaced or not.

In addition, for wound dressing applications, polymer nanofibers are a very well-suited matrix material. Nanofibrous nonwovens are characterized by a high specific surface area, small pore size, high pore volume and high absorbance capacity, making them ideal candidates for both advanced wound care and advanced sensor applications.[11–14] Indeed, these properties allow for fluid drainage, exchange of gases, protection against bacteria, good conformation to the contour of the wound, fast and scar-free healing, very high sensitivity to analytes and fast response time.[5,14–23] The use of pH-sensitive nanofibers could, thus, lead to dressings that simultaneously stimulate and monitor wound healing.

Currently, the most commonly applied processing technique for making halochromic nanofibers is dye-doped solvent electrospinning, which provides a relatively simple way to produce colored nanofibers by simply adding the dye to the polymer solution before electrospinning. However, previous studies have shown that the dye tends to leach out of such dye-doped nanofibers in the presence of moist, as it is only physically entrapped inside the nanofiber structure.[4,7,21,24–26] Dye-immobilization is, thus, currently a major challenge in nanofibrous sensor design. Extensive research on immobilization of pH-indicator dyes has shown that the use of a covalent linkage between dye and polymer matrix is the most efficient manner to inhibit dye-migration.[27–34]

In our previous work, we demonstrated efficient suppression of dye-leaching by the use of a dye-monomer approach, where a dye is functionalized with a polymerizable group and subsequently copolymerized with a suitable comonomer, providing a covalent linkage between dye and polymer.[4] Successful suppression of dye-leaching was achieved, except at high pH, where partial degradation of the polyacrylate ester groups led to dye-leaching. Furthermore, this dye-monomer approach is rather labor intensive as a polymerizable dye has to be prepared and purified, followed by polymerization and purification of the dye-functionalized polymer. Moreover, many dyes contain phenolic groups that will interfere and retard the radical polymerization process.

To overcome these limitations of the dye-monomer approach, the current paper reports a simpler and more versatile approach based on covalent dye-modification of a commercially

[a] Fibre and Colouration Technology Research Group, Department of Textiles, Faculty of Engineering and Architecture, Ghent University (UGent), Technologiepark 907, 9052 Ghent, Belgium – +32 (0)9 264 57 40 – karen.declerck@ugent.be
[b] Supramolecular Chemistry Group, Department of Organic and Macromolecular Chemistry, Faculty of Sciences, Ghent University (UGent), Krijgslaan 281 S4, 9000 Ghent, Belgium – +32 (0)9 264 44 82 – richard.hoogenboom@ugent.be
†Electronic Supplementary Information (ESI) available: (1) ^{1}H-NMR spectra, (2) Dye-modification of chitosan, (3) Electrospinning of dye-containing nanofibers. See DOI: 10.1039/x0xx00000x

available biopolymer backbone using its reactive side groups, followed by blend electrospinning with an easy-to-spin polymer as bulk matrix. The covalent modification is performed via an amide linkage to overcome the base hydrolysis that was previously reported when using polyacrylates.[4] This new strategy is generally applicable for any sensor design, but is of particular interest when using natural (bio)polymers for biomedical use as these are mostly biocompatible and can exhibit biological activity on the one hand while carrying many functional groups in the side chain on the other hand.[35] The nanofibrous structure is ideally produced via blend electrospinning allowing the selection of a suitable carrier polymer that is widely available and well electrospinnable. In addition, blend electrospinning of a matrix polymer with an appropriate amount of dye-functionalized polymer for the specific application lowers the required amount of the more expensive dye-functionalized polymer.

Here, poly(ε-caprolactone) (PCL) was chosen as a matrix polymer, instead of polyamide-6 used in our previous paper, in order to obtain a blend suitable for biomedical applications as PCL is biocompatible and biodegradable.[36–42] Chitosan is chosen as the polymer for dye-functionalization and will be modified via its amino-groups to provide for the halochromic function. Due to its availability, biodegradability, biocompatibility, sterilizable and antibacterial properties, chitosan is very well-suited for the intended biomedical sensor application.[6,43–49] Furthermore, chitosan has already been successfully blend-electrospun in previous studies.[21,43,50–53]

For the chitosan modification, Methyl Red (MR) is chosen as representative for the azo-dyes, because it is one of the most commonly applied pH-indicators. Additionally, Rose Bengal is chosen as a representative for the xanthene-dyes and is often used in biomedicine due to its ability to produce singlet oxygen by the influence of UV-light. Importantly, both selected halochromic dyes possess a functional carboxyl-group that is available for coupling with chitosan, without disrupting the chromophore, i.e. leaving halochromism intact, which is key in the dye-selection.[54–65]

Within this work, we aim to design smart, biocompatible, halochromic nanofibers, free of dye-leaching, in a universal manner, without negatively affecting the electrospinning process. Therefore, the potential of the proposed covalent dye-modification strategy is first studied by analysis of the solubility and electrospinning behavior of the dye-chitosan/PCL polymer blend solutions. Secondly, the migration and halochromic behavior of the produced nanofibers is investigated by comparison of this behavior to dye-doped PCL/chitosan nanofibers.

Experimental

Instruments and materials

Medium molecular weight chitosan (Cs, degree of deacetylation of 80.7% by potentiometric titration, average Mv of 231 kg.mol-1) and polycaprolactone (PCL, average Mn of 80 kg.mol-1) were purchased from Sigma-Aldrich. Methyl Red (MR) was also obtained from Sigma-Aldrich, whereas Rose Bengal (RB) was supplied by TCI.

Solvents used for electrospinning included acetic acid (AA, 99.8 v%) and formic acid (FA, 98.0 v%) supplied by Sigma-Aldrich. For dye-modification of chitosan, EDC.HCl and HOBt.H2O were obtained from Iris Biotech GmbH, ethanol absolute (EtOH) provided by VWR Chemicals and tetrahydrofuran (THF, 99.9 v%) was received from Sigma-Aldrich. For NMR analysis, deuterated tetrafluoroacetic acid (TFA-d, 99.5 v%) was obtained from Sigma-Aldrich. For the dye-responsive and dye-leaching tests, the following materials were used: water baths with pH adjusted using hydrochloric acid (HCl, 37 v%) and an aqueous solution of sodium hydroxide (NaOH, 50 wt%) supplied by Sigma-Aldrich, vapors of hydrochloric acid (HCl, 37 v%) and liquid ammonia (NH3, 25 v%) supplied by Sigma-Aldrich, and adjacent reference fabrics (polyamide and wool) purchased from James Heal (meeting requirements of ISO 105-F03 and ISO 105-F01 respectively).

Dye-modification of chitosan

Chitosan functionalization was executed following the method described by Fangkagwanwong et al., using either MR or RB in different concentrations (5, 10 or 20 mol% with respect to free amine groups).[66] In order to improve solubility, HOBt.H_2O (2 eq) was added to chitosan (1 eq) in deionized water at room temperature, while the solution was stirred vigorously. The reaction was left to stir overnight at 50 °C. The dye (0.05, 0.1 or 0.2 eq) was dissolved in THF and added to the solution. EDC (2 eq), dissolved in ethanol, was added dropwise. The reaction was left to stir overnight. After the ethanol and THF were evaporated under reduced pressure and the pH was raised to 10 by the addition of NaOH, the insoluble fraction inside this mixture was separated by centrifugation and ultrasonically washed with deionized water, after which a gel-like structure was obtained. The remaining water was removed by freeze-drying, after which a fine powder was produced. The remaining unreacted dye was removed by extraction with ethanol using a Soxhlet setup.

^{1}H-NMR spectra were recorded with a Bruker Avance 500 MHz spectrometer at room temperature in deuterated TFA. The amount of MR present on the chitosan polymer backbone is estimated as the ratio of the peak area between 8.5 and 7.5 ppm (accounting for 8 protons corresponding to the aromatic structure of MR) and the peak area at 3.6 ppm (acetal proton present on Cs monomers). In the case of modification with RB, the amount of dye coupled to the chitosan backbone was estimated as the ratio of the peak area between 8.9 and 7.85 ppm (both accounting for 1 proton corresponding to the aromatic structure of RB) and the integration of the 3.6 ppm peak (acetal proton present on Cs monomers). It should be noted that results are indicative as the NMR-data may show a significant error due to peak overlap of the polymer signals (ESI1-3†).

Electrospinning

The dye-containing nanofibers were produced on a rotating drum electrospinning setup with low drum speed using the

solvent electrospinning technique. This allowed for production of large nonwoven membranes (1600 cm^2).

All electrospinning trials were carried out using an 18 gauge stainless steel mixing needle without bevel (Nordson EFD), a flow rate of 0.4 $ml.h^{-1}$ and a tip-to-collector distance of 8 cm, with the voltage adapted for stable electrospinning and ambient parameters of 21 ± 2°C and 45 ± 5% RH. All electrospinning solutions contained 7 wt% of polymer in 30/70 AA/FA with an 85/15 polymer ratio of PCL to (dye-functionalized) chitosan, unless specifically stated otherwise. In parallel to the samples containing the dye-modified chitosan batches, also dye-doped nanofibers were produced by adding MR or RB directly to the electrospinning solution in the same concentration.

Prior to electrospinning, the polymer solutions were characterized by their viscosity and conductivity, using a Brookfield viscometer LVDV-II (spindle S18, viscosity range of 1.5 – 30,000 mPa.s) and a CDM210 conductivity meter (Radiometer Analytical) respectively. The standard deviations for these measurements were on average 8% and 11%.

Characterization of the electrospun nanofibers

The electrospun samples were analyzed by an FEI Quanta 200 F FE-SEM at an accelerating voltage of 20 kV. Samples were prepared prior to analysis by applying a gold coating using a sputter coater (Balzers Union SKD 030). The nanofiber diameters were measured using ImageJ. The average diameters and their standard deviations were based on 50 measurements per sample.

All color measurements were performed using a double beam UV-Vis spectrophotometer (Perking-Elmer Lambda 900). Solutions were measured in transmission using 1 cm matched quartz cells, and solid samples were measured in reflection using an integrated sphere (Spectralon Labsphere 150 mm). Spectra were recorded between 200 nm and 800 nm with a data interval of 1 nm (transmission) and 4 nm (reflection). Transmission and reflection are converted into absorbance (A) and Kubelka-Munk (K-M) respectively, providing a correlation with dye-concentration. Halochromic behavior was tested by immersion of the samples in water baths of which the pH was adjusted using HCl, NaOH and a combined reference and glass electrode (SympHony Meters VMR).

Details on the dye-migration/immobilization characterization methodology is described in our previous work.[4] Dye-leaching and dye-migration of the nanofibrous samples to respectively aqueous environment and reference fabrics were tested, and this for several pH values. Dye-leaching can be evaluated using the absorbance values of the pH baths (A) after 24 hour immersion of the dye-containing nanofibers. The pH baths were made alkaline, *i.e.* pH 12, before UV-Vis analysis for a correct comparison between the absorbance values. Dye-migration includes the staining of reference fabrics (expressed as a color difference with respect to the unstained reference; ΔE) after being in contact with the dye-containing nanofibers in a moist environment.

Results and Discussion

Dye-modification of chitosan

The covalent modification of chitosan is first performed, providing the polymer with a stable halochromic function. Chitosan is easily modified via its amino-group that can be coupled to the carboxyl-group present on the dye resulting in a stable amide linkage (Figure 1). It is of utmost importance that a dye is selected, of which the reactive group for modification is not essential in the halochromic mechanism to retain the pH-sensitivity and associated color change, which is the case for both MR and RB (Figure 2).

For MR, three batches were prepared, each with a different dye-concentration, *i.e.* Cs-MR_5 by the addition of 5 mol% MR, Cs-MR_{10} by the addition of 10 mol% MR and Cs-MR_{20} by the addition of 20 mol% MR, leading to light colored and more bright colored powders respectively (Figure 2a and ESI4†). As expected the amount of coupled dye increases with increasing dye-concentration in the reaction, but it is also evident that with increasing dye-concentration the coupling efficiency also increases (Table 1). This latter observation may be an effect of improved solubility of chitosan when some dyes are coupled, making it easier to couple more dyes.

In case of RB, two batches were prepared according to the same procedure as the MR-modification. Both were based on the addition of 10 mol% RB, whereby the first reaction was performed for 16 hours and the second for 24 hours, leading to pink colored powders with increased brightness for the second batch corresponding to a higher amount of RB-incorporation (Figure 2b and ESI4†).

Electrospinning

The polycationic nature of chitosan in solutions gives rise to very high viscosities, even at very low concentrations, which compromises electrospinnability of the polymer. Blending with a well-electrospinnable carrier polymer is one of the most straightforward ways to produce chitosan-containing nanofibers in a stable and scalable manner.[21,43,47,50,52,53,67–69] Therefore, blend electrospinning was performed by adding PCL to the polymer solution as a carrier agent.

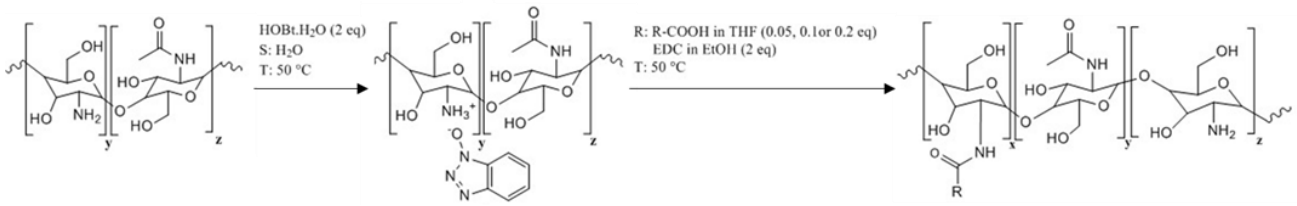

Figure 1. General mechanism for modification of chitosan with a dye possessing a functional carboxyl-group (R-COOH).

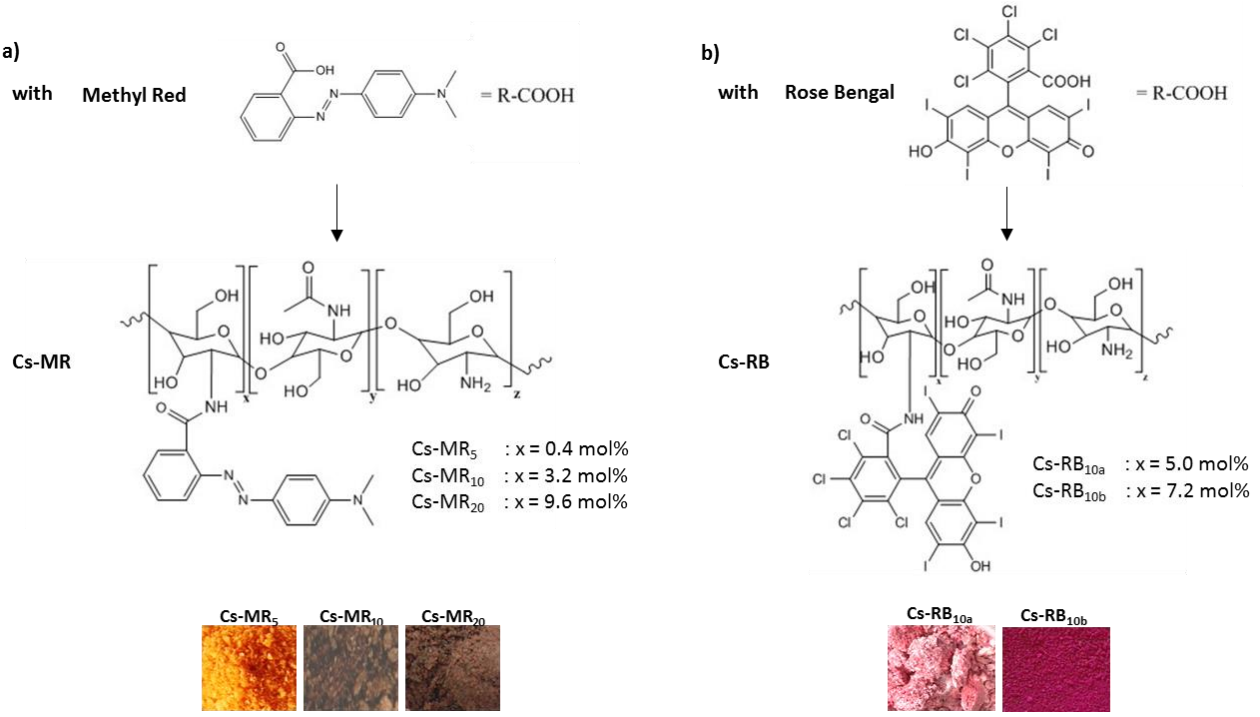

Figure 2. Modification of chitosan with a) Methyl Red and b) Rose Bengal resulting in red and pink colored powders, respectively, with brightness depending on dye-concentration.

Table 1. Characteristics of the produced batches of dye-modified chitosan. Three batches were produced with Methyl Red and indicate a higher reaction efficiency at higher dye-concentrations. Two batches were produced with Rose Bengal and indicate a higher reaction efficiency with Rose Bengal compared to Methyl Red by the addition of 10 mol% dye.

	Cs-MR_5	Cs-MR_{10}	Cs-MR_{20}	Cs-RB_{10a}	Cs-RB_{10b}
Dye concentration for modification	5 mol% MR	10 mol% MR	20 mol% MR	10 mol% RB	10 mol% RB
Reaction efficiency	8 %	32 %	48 %	50 %	72 %
Final dye concentration	0.4 mol% MR	3.2 mol% MR	9.6 mol% MR	5.0 mol% RB	7.2 mol% RB

The biocompatible PCL is well-electrospinnable using solvent systems with limited toxicity, and has already shown to be suitable for blend electrospinning with chitosan, resulting in uniform bead-free nanofibers suitable for biomedical and sensor applications.[21,51–53,39] Additionally, blending PCL and chitosan combines several desired properties, such as improved mechanical strength compared to pure chitosan nanofibers and improved wettability compared to pure PCL nanofibers.[21,51,53,37,40] By substituting the pure chitosan powder for a dye-functionalized chitosan powder in the blend electrospinning process, nanofibrous membranes are produced containing covalently immobilized MR or RB.

The electrospinnability of the PCL/Cs-MR and PCL/Cs-RB blend solutions was studied as a function of dye concentration, processing conditions, process stability and resulting fiber morphology. These results were subsequently compared to pure and dye-doped PCL/Cs solutions.

Dye-doping of the polymer blend solution does not significantly affect the electrospinning process and leads to uniform bead-free nanofibers for all tested dye-concentrations (ESI4†). This is in line with previous studies on dye-doping of electrospun fibers.[4,21,25,26,70–73]

Modification of chitosan with a dye, on the other hand, has a major effect on the electrospinnability.

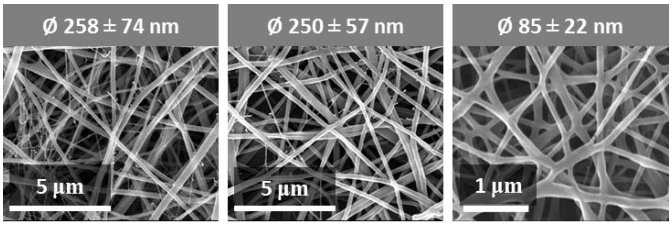

Figure 3. SEM-images of pure chitosan (left), MR-modified chitosan (middle) and RB-modified chitosan (right) blend electrospun with PCL. RB-modified chitosan nanofibers show a much lower fiber diameter than MR-modified and pure chitosan nanofibers as a result of the increased solubility and, therefore, decreased viscosity of chitosan after modification.

When only a small amount of chitosan's amino-groups are occupied by MR, which is the case for PCL/Cs-MR_5, the blend solution remains well electrospinnable without any significant changes in process stability or fiber morphology (Figure 3).

With increasing MR concentration, however, the solubility of the dye-modified chitosan powder is tremendously affected.

Both the Cs-MR_{10} and the Cs-MR_{20} batch no longer completely dissolve in the applied formic acid/acetic acid solvent system, possibly due to double protonation of the MR dye, and the blend solutions are no longer electrospinnable (ESI4†). In the case of RB, on the other hand, dye-modification substantially improves the processability of chitosan. The PCL/Cs-RB_{10a} polymer blend solutions show a spectacular drop in viscosity, due to the increased solubility of chitosan in the applied solvent system after modification with RB. This is possibly due to the decrease in polymer charge and/or the bulkiness of RB that can suppress interpolymer interactions, resulting in a very small nanofiber diameter (± 85 nm, Figure 3c). Even at a higher RB-concentration, *i.e.* PCL/Cs-RB_{10b}, the polymer blend solutions remain well electrospinnable, albeit requiring an adjusted PCL/Cs-RB ratio, *i.e.* 95/5 instead of 85/15, leading to a lower viscosity and, thus, decreased nanofiber diameter (ESI4†).

This case study, thus, indicates that even a small amount of dye covalently coupled to the chitosan, can significantly change the solubility and polycationic behavior of chitosan in the acidic electrospinning solution, which, in turn, affects electrospinnability. Selection of a suitable dye should, thus, not only take the halochromic properties into account, but also the effect on solubility and subsequent electrospinnability of the dye-modified chitosan powder.

Halochromic properties and dye-immobilization

The effect of covalent linking to chitosan on the halochromic behavior of the dyes was studied by comparison of the dye-modified chitosan nanofibers with dye-doped chitosan nanofibers and the dyes in aqueous solution.

Although only lightly colored at low dye-concentrations, the MR-containing nanofibers all show a color change from pink to yellow with increasing pH, similar to MR in aqueous solution (Figure 4a and ESI5†).

The RB-containing nanofibers show an increase in the color intensity of pink with increasing pH, also similar to RB in solution (Figure 4b and ESI5†). This indicates that the immobilization of the dyes through covalently bonding to chitosan does not impede the (de)protonation of the dyes and their corresponding halochromic behavior.

The color change is reversible and fast; all the dye-containing PCL/Cs membranes changed color within one minute. Additionally, the sensing behavior is not only observed in aqueous media, but also when being exposed to hydrochloric acid or ammonia vapors, and this with an instantaneous response.

A quantative characterization of the halochromic behavior is possible through UV-Vis spectroscopy, as shown in Figure 5. The nanofibrous samples were immersed in water baths with pH varying between 0 and 12 prior to the measurement. Normalized Kubelka–Munk spectra of the samples show that both the dye-doped membranes and the membranes containing dye-modified chitosan are characterized by a color change due to a shift to lower wavelengths, *i.e.* a hypsochromic shift, in the case of MR and a decrease in color intensity in the case of RB. The disappearance of color for RB-modified chitosan at low pH-values can be subscribed to the formation of a lactam-configuration, which is also observed with Rhodamine. This structure is similar to the lactone-structure of unmodified RB in solution, which disrupts the xanthene-chromophore, resulting in the loss of color (Figure 6).[54–62,64,74–78] The color does not completely disappear for the RB-modified nanofibers, as is the case for RB in solution and RB-doped nanofibers, possibly due to the hydrophobic nature of the polycaprolactone nanofibers present. However, a clear change in color intensity is visible to the naked eye.

Although the peak maxima for the MR-containing nanofibers are slightly shifted with respect to MR in aqueous solution, the differences are only minor (≤ 5 nm) and the color change of the dye-containing nanofibers is comparable to the dyes in solution.

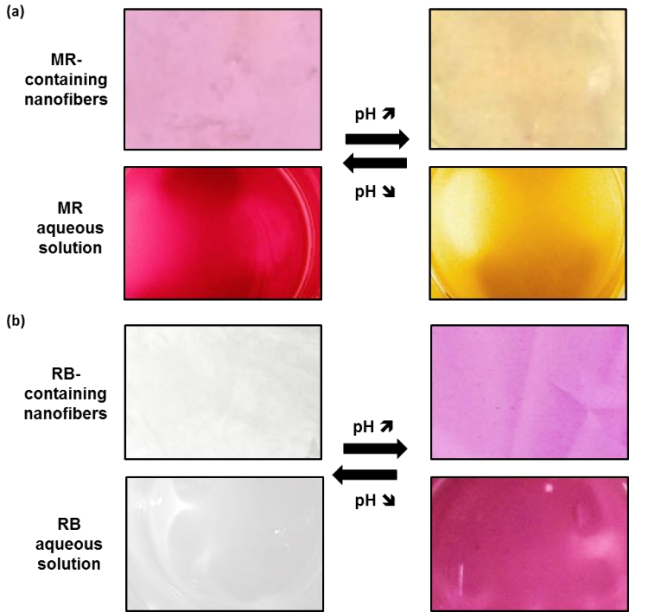

Figure 4. Methyl Red possesses a color change from red to yellow with increasing pH of aqueous solution. b) Rose Bengal possesses a color change from colorless to pink with increasing pH of aqueous solution. In both cases, this behavior is largely maintained if the dye is incorporated within a nanofibrous structure, which indicates that the covalent incorporation is not detrimental to the halochromic mechanism of the dye.

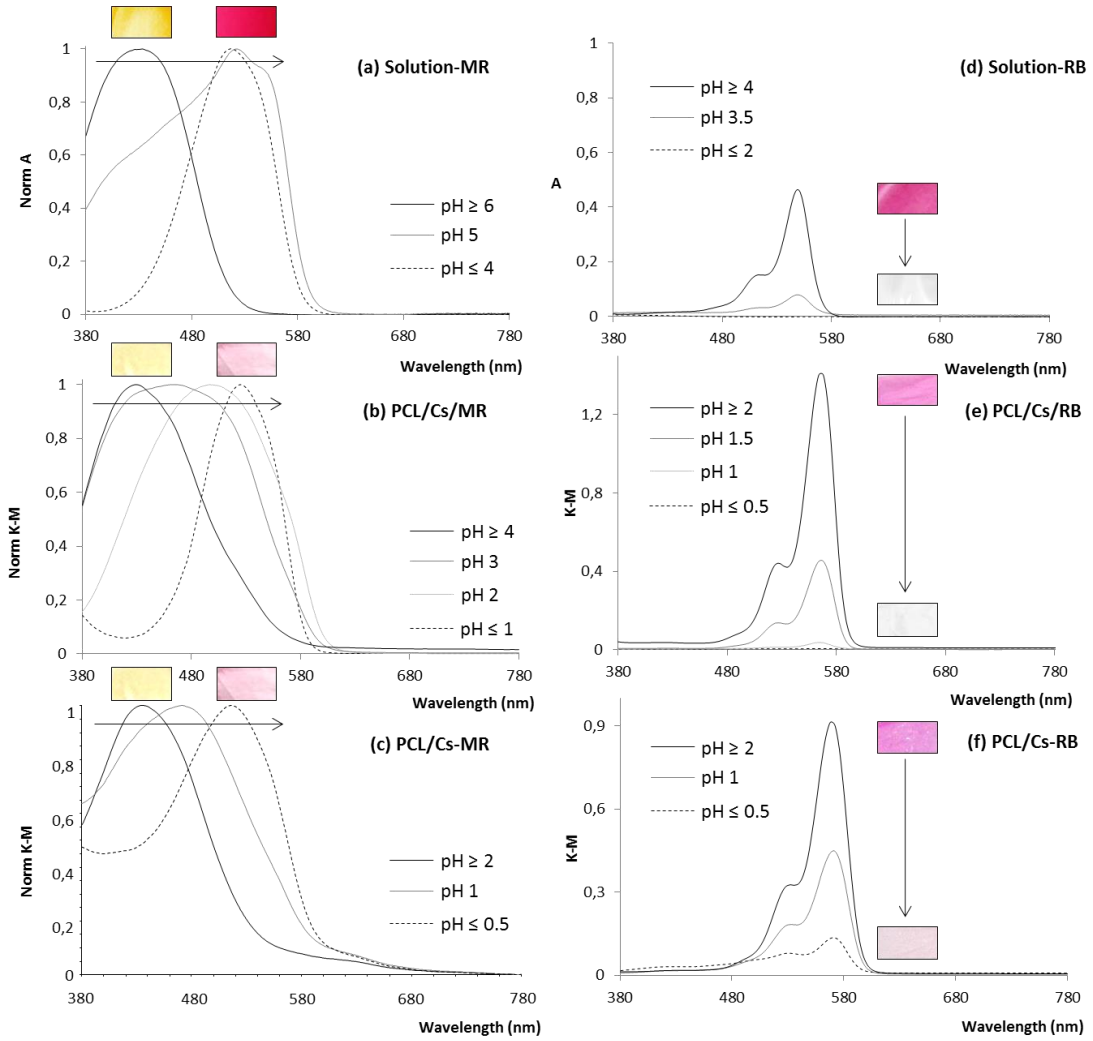

Figure 5. UV-Vis spectra show similar halochromic behavior of dye-doped and dye-modified nanofibers as the dyes in solution, except for a decrease in dynamic pH-range due to the presence of the polymer structure. The covalent modification, thus, leaves the halochromic behavior of the dyes intact. In case of MR the halochromic behavior consists of a hypsochromic shift with increasing pH. For Rose Bengal the halochromic behavior consists of an increase in color intensity with increasing pH. The RB-modified nanofibers do not become completely colorless, possibly due to the presence of the hydrophobic PCL nanofibers, keeping part of the dye-molecules shielded from water. (For RB-modified nanofibers, results were based on PCL/Cs-RB_{10b} as PCL/Cs-RB_{10a} showed similar results)

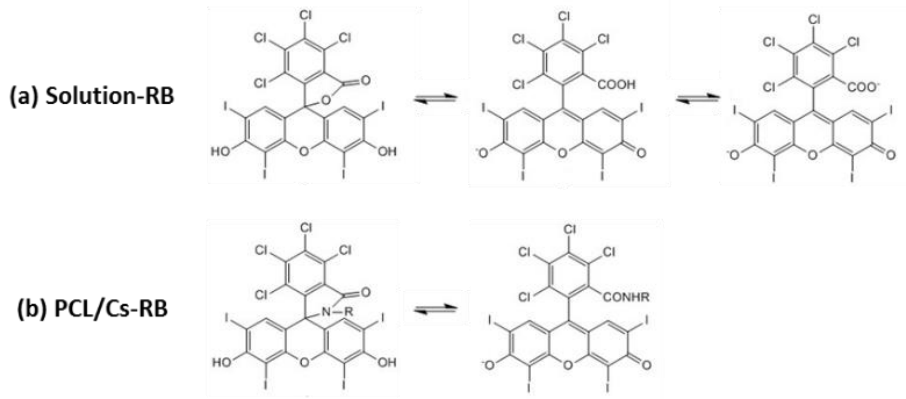

Figure 6. Mechanism of (de)protonation for a) RB in solution explaining the loss of color in acidic environments by the presence of the lactone configuration. A similar mechanism, *i.e.* lactam configuration, explains the decrease in color intensity in acidic environments in case of b) RB-modified chitosan

In case of the RB-containing nanofibers, however, the peak maxima are bathochromically shifted with 20 nm with respect to RB in solution, possibly due to the presence of the polymer matrix. This difference, however, is not visible to the naked eye. In contrast to the color shift itself, the dynamic pH-range is significantly affected by a change in microenvironment. Indeed,

both MR-doped and RB-doped PCL/Cs nanofibers change color at lower pH-values compared to MR or RB in solution (Figure 5). This is due to possible dye-matrix interactions, such as hydrogen bonding and ionic interactions, and has also been observed with other dye/polymer systems.[4,21,24,70,79] A further decrease of the dynamic pH-range is recorded when MR is covalently bonded to the polymer matrix, ascribed to transformation of the carboxylic acid group into an amide, which leads to a change in interactions with the azo-group and a pKa-shift, as has already been described in literature (Figure 5).[79] While the changes to the carboxyl group of MR and RB upon modification of chitosan do not significantly change the colors of the dyes, a more acidic environment is, thus, needed in order to protonate the dyes.

The efficiency of covalent dye-immobilization is tested by investigating the leaching of the dye towards an aqueous bath of certain pH and staining of a reference fabric in contact with the dye-modified nanofibers in moist environments of certain pH, *i.e.* dye-migration. These results are compared to the leaching and migration behavior of dye-doped nanofibers containing the same dye-concentration as the dye-modified nanofibers.

The results clearly show that dye-leaching and dye-migration significantly decreased upon covalent attachment in comparison to dye-doped nanofibers, as for both dye-doped samples a strong dye-leaching and dye-migration is observed over the entire pH-region. For the dye-doped samples the pH of the medium affects the dye-leaching and migration results as this alters the dye-solubility and dye-affinity for the reference fabric. In contrast, for both covalent dye-modified samples, dye-leaching to the water bath is almost non-existent for the full pH-range from pH 2 up to pH 12. Additionally, the MR-modified nanofibers show no dye-migration to the reference fabric over the entire pH-range.

Similarly, the RB-modified nanofibers show almost no dye-migration to the reference fabric, except for a very minor amount at pH 11 and pH 12. This is probably due to a small fraction of remaining unreacted RB in combination with a high affinity of RB for the reference fabric; the latter can be concluded from the very high dye-migration values observed for the dye-doped samples at high pH. To our knowledge, halochromic nanofibers that are stable at pH-values ranging from very acidic (pH 2) to very basic (pH 12) have not been reported before. Our own previous studies commonly showed a higher dye-leaching at high pH-values, either due to polymer degradation or due to hydrolysis and solubility of the dye-monomer linkage.[4,80]

The pH-region pH 6-10, is particularly important for biomedical applications.[1–5,7,8,10] Here, the RB-modified and MR-modified nanofibers remain fully intact, even up to pH 12, indicating efficient dye-immobilization by the covalent dye-modification, resulting in a stable halochromic nanofibrous material, which is highly relevant for biomedical applications

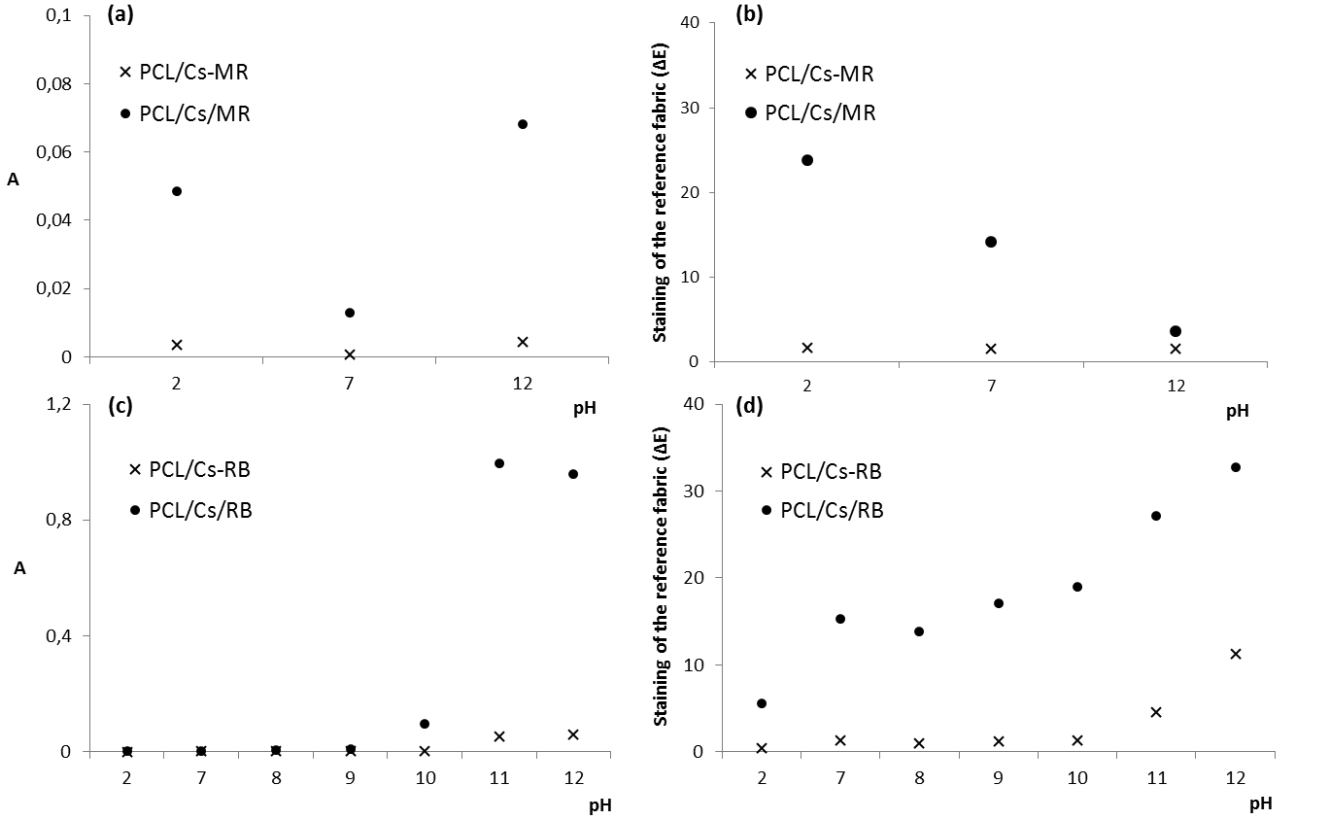

Figure 7. Comparison of leaching towards water baths (left) and migration towards reference fabrics (right) between dye-doped and dye-modified nanofibers, indicates efficient impediment of dye-release when the dye is covalently coupled to the polymer backbone. In case of the dye-doped nanofibers, the migration is dependent on the medium, *i.e.* much less dye migrates towards the neutral water baths at pH 7-9 due to the low solubility of the dyes in neutral water and much less MR migrates towards the reference fabrics due to the low affinity of polyamide for MR at this pH. For Rose Bengal, dye-doped nanofibers show no migration at pH 2.

Conclusions

Within this work, covalent dye-modification is presented as an attractive alternative strategy to the commonly applied dye-doping technique for the production of colorimetric nanofibrous sensors, as dye-doped samples frequently suffer from dye-leaching. Here, the introduction of halochromism into nanofibers was successfully executed by the covalent modification of chitosan with two halochromic dyes from commonly used dye-classes, *i.e.* azo-dyes and xanthene-dyes, before blend electrospinning. Albeit with electrospinnability depending on the dye, biocompatible, fast responding, halochromic nanofibers were fabricated that instantaneously respond to pH-changes in both aqueous solution and when exposed to acidic or basic gases. Covalent dye-modification was proven to be a viable dye-immobilization strategy, since the dyes were fully immobilized in the biomedical relevant pH-region, with only minor changes in their halochromic properties. Stable halochromic nanofibers show potential in many fields such as protective clothing, agriculture and biomedicine. For the latter, and wound management in particular, future research will include a broadening of the selection of suitable dye-matrix combinations towards color changes in the pH-range within the neutral to alkaline pH-region, as this is the pH-range accompanied with wound healing. The results given here already paved the road for covalent dye-modification combined with blend electrospinning, which has major potential, particularly, in the area of natural (bio)polymers, as it provides a universal method for versatile dye-functionalization of large area nanofibrous membranes, accompanied with proper dye-immobilization.

Acknowledgements

Financial support from The Agency for Innovation by Science and Technology of Flanders (IWT) is gratefully acknowledged. Results in this paper were obtained within the framework of the IWT Strategic Basic Research grants 111158, 111141 and 121241.

Notes and references

1 R. Christie, *Colour Chemistry*, Royal Society of Chemistry, 2014.

2 K. Devarayan and B.-S. Kim, *Sensors Actuators B Chem.*, 2015, **209**, 281–286.

3 R. W. Sabnis, *Wiley: Handbook of Biological Dyes and Stains: Synthesis and Industrial Applications*, 2010.

4 I. Steyaert, G. Vancoillie, R. Hoogenboom and K. De Clerck, *Polym. Chem.*, 2015, **6**, 2685–2694.

5 L. Van der Schueren and K. De Clerck, *Text. Res. J.*, 2009, **80**, 590–603.

6 L. A. Andrady, *Science and Technology of Polymer Nanofibers*, 2008.

7 T. R. Dargaville, B. L. Farrugia, J. a. Broadbent, S. Pace, Z. Upton and N. H. Voelcker, *Biosens. Bioelectron.*, 2013, **41**, 30–42.

8 G. Gethin, *Wounds UK*, 2007, **3**, 52–56.

9 M. Romanelli, G. Gaggio, M. Coluccia, F. Rizzello and A. Piaggesi, *Wounds*, 2002, **14**.

10 G. Schoukens, in *Advanced Textiles for Wound Care*, Woodhead, 2009, vol. 85, pp. 114–152.

11 A. L. Andrady, *Science and Technology of Polymer Nanofibers*, John Wiley & Sons, 2008.

12 S. Virji, J. Huang, R. B. Kaner and B. H. Weiller, *Nano Lett.*, 2004, **4**, 491–496.

13 X. Wang, C. Drew, S.-H. Lee, K. J. Senecal, J. Kumar and L. A. Samuelson, *Nano Lett.*, 2002, **2**, 1273–1275.

14 C. Wolf, M. Tscherner and S. Köstler, *Sensors Actuators B Chem.*, 2015, **209**, 1064–1069.

15 S. Ather and K. G. Harding, in *Advanced Textiles for Wound Care*, ed. S. Rajendran, 2009, pp. 3–19.

16 N. Bhattarai, D. Edmondson, O. Veiseh, F. A. Matsen and M. Zhang, *Biomaterials*, 2005, **26**, 6176–84.

17 A. Gefen, M. W. Carlson, S. Dong, J. A. Garlick and C. Egles, in *Bioengineering Research of Chronic Wounds*, 2009, vol. 1, pp. 263–280.

18 Y.-F. Goh, I. Shakir and R. Hussain, *J. Mater. Sci.*, 2013, **48**, 3027–3054.

19 M. Prabaharan, R. Jayakumar and S. V. Nair, in *Biomedical Applications of Polymeric Nanofibers*, eds. R. Jayakumar and S. Nair, Springer Berlin Heidelberg, Berlin, Heidelberg, 2012, pp. 140–262.

20 S. Schreml, R.-M. Szeimies, L. Prantl, M. Landthaler and P. Babilas, *J. Am. Acad. Dermatol.*, 2010, **63**, 866–881.

21 L. Van Der Schueren, T. De Meyer, I. Steyaert, Ö. Ceylan, K. Hemelsoet, V. Van Speybroeck and K. De Clerck, *Carbohydr. Polym.*, 2013, **91**, 284–293.

22 F. J. Vermolen and E. Javierre, in *Bioengineering Research of Chronic Wounds*, ed. A. Gefen, Springer Berlin Heidelberg, Berlin, Heidelberg, 2009, vol. 1, pp. 127–168.

23 C. Weller, in *Advanced Textiles for Wound Care*, ed. S. Rajendran, 2009, pp. 97–113.

24 L. Van Der Schueren, K. Hemelsoet, V. Van Speybroeck and K. De Clerck, *Dye. Pigment.*, 2012, **94**, 443–451.

25 A. Agarwal, A. Raheja, T. S. Natarajan and T. S. Chandra, *Sensors Actuators, B Chem.*, 2012, **161**, 1097–1101.

26 I. Steyaert, H. Rahier and K. De Clerck, in *Electrospinning for High Performance Sensors*, eds. A. Macagnano, E. Zampetti and E. Kny, 2015, pp. 157–177.

27 T. Carofiglio, C. Fregonese, G. J. Mohr, F. Rastrelli and U. Tonellato, *Tetrahedron*, 2006, **62**, 1502–1507.

28 T. Doussineau, A. Schulz, A. Lapresta-Fernandez, A. Moro, S. Körsten, S. Trupp and G. J. Mohr, *Chemistry*, 2010, **16**, 10290–9.

29 A. Lobnik, I. Oehme, I. Murkovic and O. S. Wolfbeis, *Anal. Chim. Acta*, 1998, **367**, 159–165.

30 P. Makedonski, M. Brandes, W. Grahn, W. Kowalsky, J. Wichern, S. Wiese and H.-H. Johannes, *Dye. Pigment.*, 2004, **61**, 109–119.

31 G. J. Mohr, H. Müller, B. Bussemer, A. Stark, T. Carofiglio, S. Trupp, R. Heuermann, T. Henkel, D. Escudero and L. González, *Anal. Bioanal. Chem.*, 2008, **392**, 1411–8.

32 T. H. Nguyen, T. Venugopala, S. Chen, T. Sun, K. T. V. Grattan, S. E. Taylor, P. A. M. Basheer and A. E. Long, *Sensors Actuators B Chem.*, 2014, **191**, 498–507.

33 S. Trupp, M. Alberti, T. Carofiglio, E. Lubian, H. Lehmann, R. Heuermann, E. Yacoub-George, K. Bock and G. J. Mohr, *Sensors Actuators B Chem.*, 2010, **150**, 206–210.

34 L. Van der Schueren, K. De Clerck, G. Brancatelli, G. Rosace, E. Van Damme and W. De Vos, *Sensors Actuators B Chem.*, 2012, **162**, 27–34.

35 C. Pietsch, U. S. Schubert and R. Hoogenboom, *Chem. Commun. (Camb).*, 2011, **47**, 8750–65.

36 N. Bölgen, Y. Z. Menceloğlu, K. Acatay, İ. Vargel and E. Pişkin, *J. Biomater. Sci. Polym. Ed.*, 2005, **16**, 1537–1555.

37 A. Cipitria, A. Skelton, T. R. Dargaville, P. D. Dalton and D. W. Hutmacher, *J. Mater. Chem.*, 2011, **21**, 9419.

38 K. W. Ng, H. N. Achuth, S. Moochhala, T. C. Lim and D. W. Hutmacher, *J. Biomater. Sci. Polym. Ed.*, 2007, **18**, 925–938.

39 L. Van Der Schueren, B. De Schoenmaker, Ö. I. Kalaoglu and K. De Clerck, *Eur. Polym. J.*, 2011, **47**, 1256–1263.

40 M. A. Woodruff and D. W. Hutmacher, *Prog. Polym. Sci.*, 2010, **35**, 1217–1256.

41 S. Reisman, A. B. Ritter, V. Hazelwood, B. B. Michniak, A. Valdevit and A. N. Ascione, *Biomedical Engineering Principles*, Taylor & Francis, 2005.

42 B. D. Ratner, A. S. Hoffman, F. J. Schoen and J. E. Lemons, *Biomaterials Science: An Introduction to Materials in Medicine*, Elsevier Science, 2012.

43 F. Croisier and C. Jérôme, *Eur. Polym. J.*, 2013, **49**, 780–792.

44 P. A. Felse and T. Panda, *Bioprocess Eng.*, 1999, **20**, 505.

45 A. Francesko, M. Díaz González, G. R. Lozano and T. Tzanov, *Developments in the processing of chitin, chitosan and bacterial cellulose for textile and other applications*, Elsevier, 2010.

46 E. Khor, in *Engineering materials for biomedical applications*, ed. T. S. Hin, 2004, pp. 11.1–11.16.

47 E. Khor, *Chitin: Fulfilling a Biomaterials Promise*, 2014.

48 G. Smart and M. R. Groocock, in *Medical Textiles and Biomaterials for Healthcare*, Elsevier, 2006, pp. 67–72.

49 K. Van de Velde, L. Szosland and I. Krucińska, in *Medical Textiles and Biomaterials for Healthcare*, Elsevier, 2006, pp. 286–295.

50 M. Pakravan, M.-C. Heuzey and A. Ajji, *Polymer (Guildf).*, 2011, **52**, 4813–4824.

51 M. P. Prabhakaran, J. R. Venugopal, T. Ter Chyan, L. B. Hai, C. K. Chan, A. Y. Lim and S. Ramakrishna, *Tissue Eng. Part A*, 2008, **14**, 1787–97.

52 K. T. Shalumon, K. H. Anulekha, C. M. Girish, R. Prasanth, S. V. Nair and R. Jayakumar, *Carbohydr. Polym.*, 2010, **80**, 414–420.

53 L. Van Der Schueren, I. Steyaert, B. De Schoenmaker and K. De Clerck, *Carbohydr. Polym.*, 2012, **88**, 1221–1226.

54 C. Åkerlind, H. Arwin, F. L. E. Jakobsson, H. Kariis and K. Järrendahl, *Thin Solid Films*, 2011, **519**, 3582–3586.

55 A. D. Broadbent, *Basic principles of textile coloration*, Society of Dyers and Colourists, 2001.

56 C.-C. Chang, Y.-T. Yang, J.-C. Yang, H.-D. Wu and T. Tsai, *Dye. Pigment.*, 2008, **79**, 170–175.

57 J. C. del Valle, N. A. García and F. Amat-Guerri, *Dye. Pigment.*, 1993, **22**, 199–205.

58 J. J. M. Lamberts and D. C. Neckers, *Tetrahedron*, 1985, **41**, 2183–2190.

59 S. M. Linden and D. C. Neckers, *Photochem. Photobiol.*, 1988, **47**, 543–550.

60 R. Malik, V. K. Tomer, P. S. Rana, S. P. Nehra and S. Duhan, *Mater. Lett.*, 2015, **154**, 124–127.

61 D. C. Neckers, *J. Photochem. Photobiol. A Chem.*, 1989, **47**, 1–29.

62 A. Shrestha, M. R. Hamblin and A. Kishen, *Nanomedicine*, 2014, **10**, 491–501.

63 D. R. Waring and G. Hallas, Eds., *The Chemistry and Application of Dyes*, Springer US, Boston, MA, 1990.

64 H. R. Zhu and L. Parker, *Chem. Phys. Lett.*, 1989, **162**, 424–430.

65 H. Zollinger, *Color Chemistry: Syntheses, Properties and Applications of Organic Dyes and Pigments*, VCH, 2nd edn., 1991.

66 J. Fangkagwanwong, M. Akashi, T. Kida and S. Chirachanchai, *Macromol. Rapid Commun.*, 2006, **27**, 1039–1046.

67 H. Homayoni, S. A. H. Ravandi and M. Valizadeh, *Carbohydr. Polym.*, 2009, **77**, 656–661.

68 P. Su, C. Wang, X. Yang, X. Chen, C. Gao, X.-X. Feng, J.-Y. Chen, J. Ye and Z. Gou, *Carbohydr. Polym.*, 2011, **84**, 239–246.

69 X. Shan, F. Li, C. Liu and Q. Gao, *J. Appl. Polym. Sci.*, 2014, **131**, n/a–n/a.

70 L. Van der Schueren, T. Mollet, Ö. Ceylan and K. De Clerck, *Eur. Polym. J.*, 2010, **46**, 2229–2239.

71 S. Ramakrishna, *An Introduction to Electrospinning And Nanofibers (Google eBook)*, World Scientific, 2005.

72 L. Matlock-Colangelo and A. J. Baeumner, *Lab Chip*, 2012, **12**, 2612–20.

73 A. Camposeo, F. Di Benedetto, R. Stabile, R. Cingolani and D. Pisignano, *Appl. Phys. Lett.*, 2007, **90**, 143115.

74 Y. Yang, W. Gao, R. Sheng, W. Wang, H. Liu, W. Yang, T. Zhang and X. Zhang, *Spectrochim. Acta. A. Mol. Biomol. Spectrosc.*, 2011, **81**, 14–20.

75 Google Patents, 2008.

76 D. K. Kölmel, *Chemische Biologie von neuen zellgängigen Peptoiden und Synthese fluoriger Farbstoffe*, Logos Verlag Berlin GmbH, 2013.

77 H. N. Kim, M. H. Lee, H. J. Kim, J. S. Kim and J. Yoon, *Chem. Soc. Rev.*, 2008, **37**, 1465–72.

78 V. N. Belov, M. L. Bossi, J. Fölling, V. P. Boyarskiy and S. W. Hell, *Chemistry*, 2009, **15**, 10762–76.

79 T. De Meyer, K. Hemelsoet, V. Van Speybroeck and K. De Clerck, *Dye. Pigment.*, 2014, **102**, 241–250.

80 J. Geltmeyer, G. Vancoillie, I. Steyaert, B. Breyne, G. Cousins, K. Lava, R. Hoogenboom, K. De Buysser and K. De Clerck, *Submitt. to Adv. Funtional Mater.*, 2016.